Pure

Syddansk Universitet

Effects of cation compositions on the electronic properties and optical dispersion of indium zinc tin oxide thin films by electron spectroscopy

Tougaard, Sven Mosbæk

Published in:
Materials Research Bulletin

Publication date:
2015

Document version
Submitted manuscript

Citation for pulished version (APA):
Tougaard, S. M. (2015). Effects of cation compositions on the electronic properties and optical dispersion of indium zinc tin oxide thin films by electron spectroscopy. Materials Research Bulletin, 62, 222-231.

General rights
Copyright and moral rights for the publications made accessible in the public portal are retained by the authors and/or other copyright owners and it is a condition of accessing publications that users recognise and abide by the legal requirements associated with these rights.

- Users may download and print one copy of any publication from the public portal for the purpose of private study or research.
- You may not further distribute the material or use it for any profit-making activity or commercial gain
- You may freely distribute the URL identifying the publication in the public portal ?

Take down policy
If you believe that this document breaches copyright please contact us providing details, and we will remove access to the work immediately and investigate your claim.

Download date: 19. Apr. 2017

Materials Research Bulletin 62 (2015) 222–231

Contents lists available at ScienceDirect

Materials Research Bulletin

journal homepage: www.elsevier.com/locate/matresbu

Effects of cation compositions on the electronic properties and optical dispersion of indium zinc tin oxide thin films by electron spectroscopy

Yus Rama Denny [a], Soonjoo Seo [b], Kangil Lee [c], Suhk Kun Oh [c], Hee Jae Kang [c,*], Sung Heo [d], Jae Gwan Chung [d], Jae Cheol Lee [d], Sven Tougaard [e]

[a] Department of Electrical Engineering, University of Sultan Ageng Tirtayasa, Banten 42435, Indonesia
[b] Division of Materials Science, Korea Basic Science Institute, Daejeon 305-806, South Korea
[c] Department of Physics, Chungbuk National University, Cheongju 361-763, South Korea
[d] Analytical Engineering Center, Samsung Advanced Institute of Technology, Suwon 440-600, South Korea
[e] Department of Physics, Chemistry, and Pharmacy, University of Southern Denmark, DK-5230 Odense M., Denmark

ARTICLE INFO

Article history:
Received 10 October 2013
Received in revised form 23 September 2014
Accepted 4 November 2014
Available online 6 November 2014

Keywords:
A. Amorphous materials
B. Sputtering
B. Optical properties
C. Electron energy loss spectroscopy
D. Dielectric properties

ABSTRACT

The electronic properties and optical dispersion of indium zinc tin oxide (IZTO) films with different cation compositions were investigated by reflection electron energy loss spectroscopy (REELS). The REELS spectra of IZTO films revealed that the band gap varied with different Sn/Zn ratios and In content. The optical properties were examined with REELS data using Tougaard–Yubero model and the results were compared with the envelope of the transmission spectra obtained using a UV-spectrometer. The dispersion behavior of the refractive index from REELS results was studied in terms of the single-oscillator Wemple–DiDomenico model. The results showed that the different compositions of In/Zn/Sn caused a change in the dispersion parameters of IZTO thin films in contrast to the static values of refractive indices and dielectric constant which remained the same. Our work demonstrated that REELS is an efficient tool to study the optical properties of a material by obtaining the optical parameters.

© 2014 Elsevier Ltd. All rights reserved.

1. Introduction

Indium zinc tin oxide (IZTO) thin films have applications as transparent conducting oxide (TCO) materials that serve as the active channel of thin-film transistors (TFTs). This is due to their high performance compared to conventional TFTs based on hydrogenated amorphous silicon (a-Si:H) having high mobility (>10 $cm^2 V^{-1} s^{-1}$), low gate sub-threshold swing, and high on-off current ratio (>10^6) [1–3]. Both indium tin oxide (ITO) and IZTO thin films have been employed as transparent electrodes for flat panel displays, touch panels, organic light emitting diodes, and solar cells because they satisfy the requirements for applications such as electrical resistivity of $\sim 10^{-4}\,\Omega$ cm and optical transmittance of 85% in the visible light region [4]. In comparison to ITO thin films, IZTO thin films are preferred because of their higher electrical conductivity, higher transparency, moderate chemical stability, higher work function, and low deposition temperature [5–7]. IZTO is also cost-effective because indium is pricy and doping ZnO into ITO can decrease the use of indium by 60% without deteriorating the electrical and optical properties [8,9].

Several studies have attempted to change the electrical, optical, and structural properties of IZTO thin films by using an annealing process and/or varying the composition of Zn and Sn. A recent study reported on IZTO thin films grown by RF magnetron sputtering with two different chemical compositions [10]. In this work, the In content was fixed to 60%, while the Sn content was varied between 15% and 25%. They found that the crystallinity of an IZTO thin film increases with a higher Sn content and exhibited much lower resistivity of $3.44 \times 10^{-4}\,\Omega$cm when deposited at 400 °C. Saji and Jayaraj [11] made IZTO thin films by a co-sputtering method at room temperature (RT) with different composition ratios of Zn/In/Sn which varied from 0.05/0.56/0.39 to 0.5/0.27/0.23 and confirmed that a change in the compositions caused a change in the optical band gap which varied from 3.0 eV to 3.44 eV with increasing Zn content. They also showed that IZTO TFTs with a high performance can be realized at RT.

In this paper, we demonstrate that the electronic and the optical properties can be improved by using a lower content of In in IZTO thin films. We made two different kinds of IZTO samples with In contents of 20% and 13%, which has not been previously reported.

* Corresponding author. Tel.: +82 43 261 2275.
E-mail address: hjkang@cbu.ac.kr (H.J. Kang).

http://dx.doi.org/10.1016/j.materresbull.2014.11.015
0025-5408/© 2014 Elsevier Ltd. All rights reserved.

We investigated the effect of different compositions of In/Zn/Sn on the energy band gap and optical properties using reflection electron energy loss spectroscopy (REELS) as well as the Tougaard–Yubero model.

In fact, REELS is a convenient technique to investigate the electronic structure of a material because the low-energy-loss region reflects the structure of the valence and the conduction electron bands [12]. The electronic structure can be obtained by analyzing the energy distribution of electrons reflected from the surface of a solid using a monoenergetic primary electron beam as in REELS [13].

The most conventional methods to measure the optical properties of transparent thin films are the envelope method using transmittance (or reflectance) spectra and the interferometric analysis method [14,15]. The interferometric method with two [16] or multiple beam interferometry and prism coupling technique [15] provide precise measurements of optical parameters, but to carry out the measurements complex tools and special experimental skills are needed [14]. On the other hand, the envelope method in transmittance spectra obtained by a UV-spectrometer uses a relatively simple procedure which depends on interference fringes. In the envelope method the optical parameters are determined by analysis of the interference fringes from transmittance spectra. However some films do not show interference fringes in the UV-spectroscopic measurement. REELS is an alternative technique to analyze optical parameters of thin films and when it is used in conjunction with the Tougaard-Yubero model (QUEELS-ε(k,ω)-REELS) it can provide information about the optical parameters of a thin film [13,17]. This method determines the dielectric function of the film, and from this, the optical parameters such as the refractive index, extinction coefficient, and transmission spectra can be easily determined. The validity of this method has been proven and applied to obtain optical parameters for ultrathin gate oxide films, dielectric materials, and transparent conducting oxides [18,19].

In our study, we demonstrated that the energy band gap was changed with lower In contents of 13% and 20%, and the optical properties were analyzed in terms of a single-oscillator method proposed by the Wemple and DiDomenico dispersion relation model [32].

2. Experimental

IZTO thin films were deposited on glass substrates at RT in argon mixed with oxygen gas ($Ar:O_2$ = 15: 85) by RF magnetron sputtering with an RF power of 200 W. IZTO thin films were produced with composition ratios of In:Zn:Sn of 20:50:30 (denoted as IZTO-I), 20:56.7:23.3 (denoted as IZTO-II), and 13:60.2:26.8 (denoted as IZTO-III). The Sn/Zn ratios for IZTO-I, IZTO-II, and IZTO-III films are approximately 0.6, 0.42, and 0.45, respectively. Thus, the Sn/Zn ratios for IZTO-II and IZTO-III films are close to each other and those values are much lower than that of IZTO-I film. The thickness of all the thin films was 35 nm. All IZTO thin films were annealed at 350 °C for 1 hour in air. The REELS spectra were obtained using a VG ESCALAB 210 equipment. The REELS spectra were measured with primary electron energies of 1.0, 1.5, and 2.0 keV and the energy distribution of backscattered electrons were measured with a hemispherical electron energy analyzer operated at a constant analyzer pass energy of 20 eV. The electron incident and exit angles from the surface normal were 55° and 0°, respectively. The full width at half maximum (FWHM) of the elastic peak was 0.8 eV. The analysis of the crystal structure was carried out on a Phillips PW-1710Cu-Kα diffractometer (λ = 1541 Å) by varying the diffraction angle 2θ from 30° to 80° with an increment of 0.009°. The surface morphology including the roughness calculation of the films was performed by atomic force microscopy (AFM) from Nanofocus Inc. system with a scanning area of $2 \times 2\ \mu m^2$. The transmittance spectra of the IZTO thin films were measured by Genesys 6 model from Thermo Electron Corporation in the wavelength range of 300–1000 nm at RT at increments of 0.1 nm.

3. Results and discussions

Fig. 1 shows the REELS spectra and UV-spectroscopic results for the IZTO thin films. The results for annealed samples in Fig. 1 were

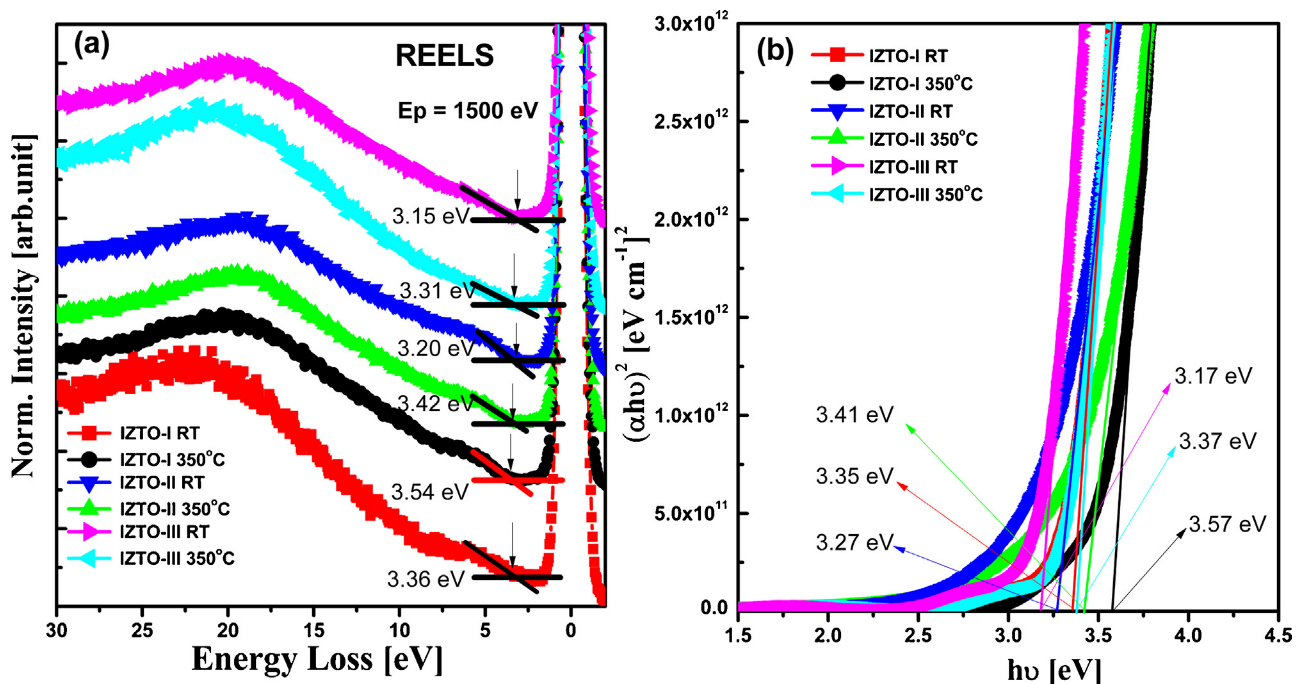

Fig. 1. (a) Reflection electron energy loss spectra with the primary energy of 1.5 keV and (b) plot of $(\alpha h\upsilon)^2$ versus $h\upsilon$ of IZTO thin films for different composition of In/Zn/Sn.

Table 1
Parameters for energy loss functions in the model of IZTO thin films as a function of different In/Zn/Sn compositions before and after annealing that give the best fit to experimental cross sections at 1.0, 1.5, and 2.0 keV.

Films	i	$\hbar\omega_{0i}$ (eV)	A_i (eV^2)	γ_i (eV)
IZTO-I-As deposited	1	7.0	0.4	8
(E_g = 3.36 eV)	2	10.0	1.8	8
(α_i = 0.05)	3	17.1	2.7	18
	4	20.6	338.5	4
	5	32.0	100.9	25
IZTO-I-350 °C	1	7.5	0.4	8
(E_g = 3.54 eV)	2	12.0	1.9	8
(α_i = 0.05)	3	17.5	2.9	18
	4	21.7	372.1	14
	5	34.0	111.0	25
IZTO-II-As deposited	1	7.0	0.6	8
(E_g = 3.20 eV)	2	8.5	2.0	7
(α_i = 0.05)	3	15.5	2.4	18
	4	20.3	339.9	15
	5	30.0	69.1	25
IZTO-II-350 °C	1	7.3	0.5	5
(E_g = 3.42 eV)	2	9.0	1.7	7
(α_i = 0.05)	3	15.9	3.0	18
	4	20.6	346.4	14.5
	5	32.0	84.8	25
IZTO-III-As deposited	1	7.0	0.2	4
(E_g = 3.15 eV)	2	8.7	1.2	8
(α_i = 0.05)	3	15.8	2.4	10
	4	20.3	355.2	14
	5	30.0	78.1	25
IZTO-III-350 °C	1	7.0	0.2	4
(E_g = 3.31 eV)	2	8.9	1.3	8
(α_i = 0.05)	3	16.2	2.5	10
	4	20.7	348.7	14
	5	31.0	81.1	25

cited in reference [21]. As shown in Fig. 1 (a), the plasmon loss peaks of IZTO-I, IZTO-II, and IZTO-III are located at around 20 eV. The REELS spectra were used to estimate the energy band gaps of the IZTO thin films by a method described in our previous work [18,19]. The results are summarized in Table 1 showing that the measured band gaps of the IZTO-I, IZTO-II, and IZTO-III thin films before annealing are 3.36, 3.20, and 3.15 eV, respectively, within an uncertainty of ±0.1 eV. The band gap was abruptly increased after annealing at 350 °C in air to 3.54, 3.42, and 3.31 eV for IZTO-I, IZTO-II, and IZTO-III thin films, respectively. For comparison, the band gap was also determined from the UV spectroscopic measurements by using the Tauc relation [20] (which is valid only for amorphous thin films). The optical band gaps were calculated on the basis of the optical spectral absorption [20], and they can be determined by extrapolating the best fit line between $(\alpha h\upsilon)^2$ and $h\upsilon$, where α, h, and υ are the absorption coefficient, the Planck's constant ($6.626 \times 10^{-34}\,m^2\,kg/s$), and the frequency of incident photons, respectively. As shown in Fig. 1 (b), the optical band gaps of the unannealed IZTO-I, IZTO-II and IZTO-III thin films were 3.35, 3.27, and 3.17 eV, respectively, and these increased to 3.57, 3.41, and 3.37 eV after annealing. The measured optical band gaps are consistent with the band gap values determined by analyzing the REELS spectra. Details about the band gap of IZTO films can be found in Ref. [21]. As can be seen in the Fig. 2 (a), all IZTO thin films show amorphous structure even for annealed films at 350 °C in air. Hence, the change of the band gap due to the annealing process cannot be related to the phase transition from amorphous to crystalline. The change in the band gap can possibly be explained by the Burstein–Moss (BM) effect [22], which describes a shift of the band gap due to much higher electron density and an increase in the filling states of the conduction band in the IZTO films. Therefore, the Fermi level moves up towards the conduction band, which leads to a shift in the energy band.

In order to investigate the optical properties of IZTO thin films, we used the envelope method for the transmission spectra from UV spectroscopic measurements and in this way the value of refractive index was calculated. Another approach to examine the optical properties was to use REELS spectra by which the optical parameters such as dielectric function, refractive index, and transmission can be determined.

In addition, we adopted another model known as Wemple and DiDomenico dispersion relation model [32] to get a complete understanding of the optical properties of the IZTO thin films. Using this method, the dispersion parameters, static refractive index, static dielectric constant, plasma oscillator energy, and the ratio of the carrier concentration to the effective mass can be obtained, which have not been reported so far in detail.

Fig. 3(a) shows the spectral transmittance of IZTO thin films deposited onto the glass substrate for unannealed and annealed films in the wavelength ranging from 300 to 1000 nm. The average transmittance of all IZTO thin films in the visible light region exceeds 87% transparency. Hence, there was no significant difference in transmittance with different Sn/Zn ratios, In contents, and the annealing process. At wavelengths below 300–400 nm, the transmission spectra show a sudden decrease due to the absorption caused by band to band electron excitations. As shown in Fig. 3(a), the interference fringes in the transmittance spectra were found in the IZTO-I and IZTO-III films, but not in the IZTO-II films. Manifacier et al. [23], and Swanepoel [24] reported that interference fringes in the transmission spectra of a thin film on a transparent substrate can give information about the optical parameters using the envelope method. Swanepoel [24] showed that interference fringes were related to the uniformity of thickness of the films. The interference effects will be destroyed and the transmission will show a smooth shape when the thickness roughness is not uniform or slightly tapered. On the other hand, the interference fringe effects give rise to the transmission spectra when the thickness is uniform [25]. The uniformity of thickness in thin films is strongly related to the homogeneity of surface morphology and surface roughness. Fig. 2(b)–(d) show the surface morphology and the root mean square (RMS) roughness of all unannealed and annealed IZTO thin films measured using AFM. The RMS roughness of IZTO-I, IZTO-II and IZTO-III films are 0.675 , 1.393, and 0.491 nm, respectively. The RMS values increased to 0.877, 1.931, and 0.549 nm for IZTO-I, IZTO-II, and IZTO-III, respectively after annealing at 350 °C (the figures were not shown). The results show that the surface roughness of IZTO-II before and after annealing was much higher than those of IZTO-I and IZTO-III films. This indicates that the reduction of interference fringes in the transmittance spectra of IZTO-II films is related to the higher surface roughness of these films.

We used these interference fringes to calculate the optical parameters of IZTO-I and IZTO-III films. The refractive index of the films was obtained by a simple method suggested by Swanepoel [24]. This method allows the calculations of the refractive index by using the maximum and the minimum envelope of the interference fringes in the transmission spectra beyond the absorption edge as follows [24]:

$$n = \sqrt{N + \sqrt{N^2 - S^2}}, \tag{1}$$

and

$$N = 2S\left(\frac{T_{max} - T_{min}}{T_{max} \times T_{min}}\right) + \frac{S^2 + 1}{2}, \tag{2}$$

where S is the refractive index of the glass substrate. T_{min} and T_{max} are the values of the envelope at the maximum and minimum transmittance, respectively, which can be obtained directly from the transmission spectra. Thus, the determined refractive indices

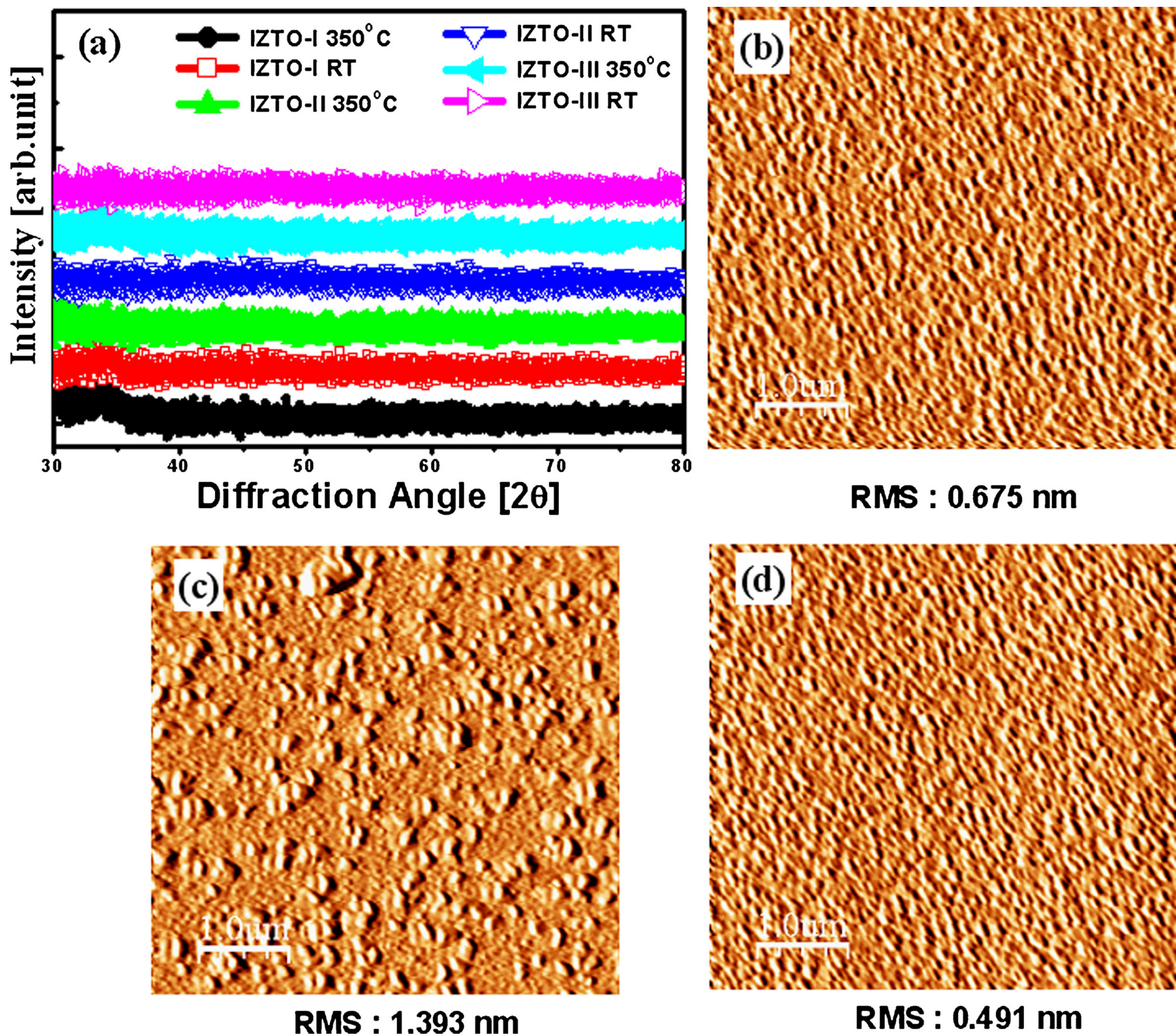

Fig. 2. (a) X-ray Diffraction pattern and Atomic Force Microscopy images of IZTO thin films deposited at room temperature for (b) IZTO-I, (c) IZTO-II, and (d) IZTO-III.

of IZTO-I and IZTO-III are 2.23 and 2.20 for unannealed films and 2.22 and 2.25 for annealed films, respectively. This result implies that there is no significant change in the refractive index with differing In contents before and after annealing. The obtained refractive indices are also in good agreement with the previous work [10].

We applied an analytical dispersion equation for the IZTO-I thin films to determine the refractive index which depended on the wavelength as described in Ref. [25]. Fig. 3(b)–(c) show the refractive index as a function of wavelength for IZTO-I films. The refractive index decreases with increasing wavelength. This result indicates that the films show a normal dispersion behavior. A similar behavior was found in IZTO-III films (which are not shown here). However, this method is not reliable to calculate the optical parameters since it needs interference fringes for analysis and not all films show interference fringes. Therefore, we employed another method, which used REELS spectra in conjunction with Tougaard–Yubero model. This analysis can give us direct information about the optical parameters of a material using the dielectric function and can be used for any materials with different surface roughness since it does not rely on interference fringes in the transmission spectra. Fig. 3(b)–(d) show a comparison between n values (for IZTO-I films) and the transmission spectra (for IZTO-II films) as a function of wavelength obtained by REELS spectra and UV spectrometric data. The results show that the REELS data agree with the UV spectrometric data.

The REELS spectra were calculated using the model of Tougaard–Yubero QUEELS-ε(k,ω)-REELS software package [13] to obtain the optical parameters of IZTO thin films. This model involves the removal of the contribution from the multiple scattered electrons from the REELS spectra determining an effective single-scattering cross section value, $K_{exp}(\hbar\omega)$, times the corresponding inelastic mean free path λ, in the form of $\lambda K_{exp}(\hbar\omega)$ [26]. The next step is to investigate the energy loss processes for the backscattered electrons which have followed different paths in the film. These energy loss processes are studied within a semi-classical dielectric response model which takes into account the variation in energy loss in the surface region. The energy loss processes were also considered, which take place when the low primary electron energies moves in the vacuum above the surface due to its interaction with its image charge [13,26,27]. Such processes are very important at the low primary electron energies applied here. The basic principle in this model is then to interpret the effective cross section derived experimentally in terms of the

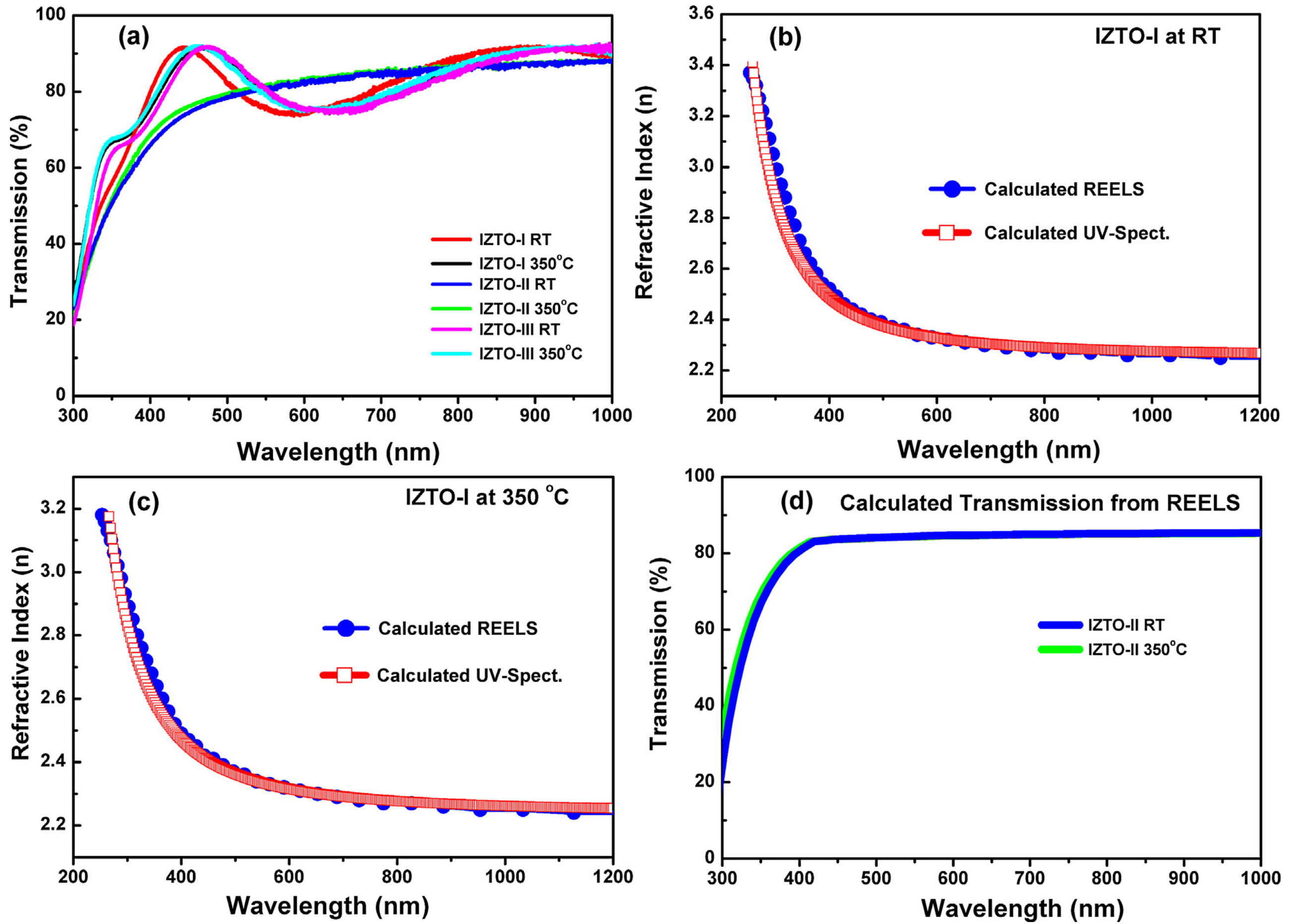

Fig. 3. (a) Transmittance spectra by UV-Spectrometer of IZTO thin films, (b-c) refractive index as a function of wavelength for IZTO-I films, and (d) calculated transmission spectra by REELS for IZTO-II films.

dielectric function ε(*k*,ω), which we parameterized by expanding the energy loss function (ELF) Im(-1/ε) in terms of Drude–Lindhard type oscillators [28]:

$$Im\left\{\frac{-1}{\varepsilon K,\omega}\right\} = \theta\hbar\omega - E_g \cdot \sum_{i=1}^{n} \frac{A_i\gamma_i\hbar\omega}{\hbar^2\omega_{oik}^2 - \hbar^2\omega^2}^2 + \gamma_i^2\hbar^2\omega^2, \quad (3)$$

in which the dispersion relation is given in the form:

$$\hbar\omega_{0ik} = \hbar\omega_{0i} + \alpha_i\frac{\hbar\omega^2K^2}{2m}, \quad (4)$$

where A_i, γ_i, $\hbar\omega_i$, and α_i are the oscillator strength, the damping coefficient, the excitation energy, and the momentum dispersion coefficient of the i_{th} oscillator, respectively while $\hbar k$ is the momentum transferred from the REELS electron to the solid. The step function $\theta(\hbar\omega$-$E_g)$ is included to simulate a possible band gap E_g, which can be estimated from the onset of the energy loss in the REELS spectrum (see Fig. 1(a)). The details of the simulated oscillators in this model were described in our previous study [13,19]. The oscillator strengths are adjusted to make sure that ε(*k*,ω) fulfils the well-established Kramer–Kronig sum rule [16,29,30]:

$$\frac{2}{\pi}\int_0^\infty Im\left\{\frac{1}{\varepsilon\hbar\omega}\right\}\frac{d(\hbar\omega)}{\hbar\omega} = 1 - \frac{1}{n^2}. \quad (5)$$

Note that *n* is the index of refraction in the static limit, and the exact value of n does not affect the result of the calculation significantly.

Fig. 4 shows the experimental λK_{exp} inelastic cross section derived from the REELS spectra. They are compared with the theoretical λK_{th} values calculated by QUEELS-ε(*k*,ω)-REELS with different In contents, Sn/Zn ratios, and annealing process. The experimental inelastic cross section was fitted with the parameter of A_i, γ_i, $\hbar\omega_i$, and α_i by a trial-and-error procedure to yield the best agreement at all primary energies of 1.0, 1.5, and 2.0 keV. The result shows a good agreement between the theoretical and experimental values for all IZTO films at all primary energies. The oscillators obtained from the REELS results for each IZTO thin film are presented in Table 1.

The energy loss functions (ELF) Im[-1/ε] and surface energy loss functions (SELF) Im[-1/(1 + ε)] of the IZTO thin films with differing In contents, Sn/Zn ratios, and the annealing process are plotted in Fig. 5(a). The ELF of the unannealed IZTO-I has originally five oscillators at 7.0, 10.0, 17.1, 20.6, and 32.0 eV, which is similar to that of the other unannealed films. The energy loss positions of the first and the fifth oscillators for the unannealed IZTO-I are almost the same as those of IZTO-II. But the second, third, and fourth oscillators of IZTO-II are shifted towards the lower energy loss positions by 1.5, 1.5, and 2.0 eV, respectively. The energy loss for the second, third and the fourth oscillators for the annealed film of IZTO-II were decreased by 3.0, 1.6, and 1.1 eV, respectively. The oscillators of IZTO-III including the energy loss position, and the widths are almost the same as those of IZTO-II. Thus, there is no difference in the electronic structure even if the In contents are reduced. This result implies that the lower Sn content and the annealing treatment have a strong effect on the electronic structure. However, a small amount of In does not cause a change

Fig. 4. Experimental inelastic cross section λK_{exp} (solid line) obtained from REELS data and the theoretical result λK_{th}(rectangle) calculated by utilizing the simulated energy loss function for primary energies of 1.0, 1.5, and 2.0 keV for IZTO thin films.

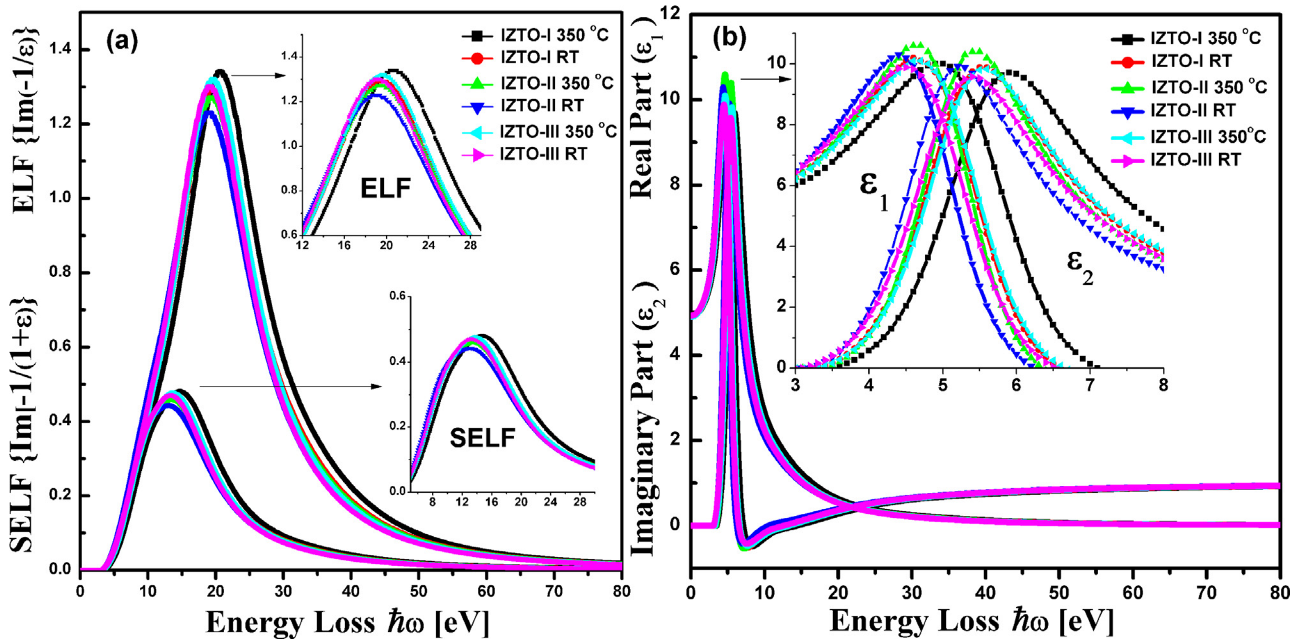

Fig. 5. (a) Energy loss functions (ELF) and surface energy loss function (SELF) calculated and (b) calculated complex dielectric function for IZTO thin films by utilizing the parameters given in Table 1.

in the electronic structure of IZTO thin films. The intensity, peak position, and shape of SELFs for all IZTO thin films are different from those of the ELFs.

The energy loss function in Eq. (3) allows us to perform a Kramers–Kronig transformation to calculate the real part of the reciprocal of the energy loss function. The real part ε_1 and imaginary part ε_2 of the dielectric function can then be calculated from Im{-1/ε} and Re{1/ε} [29,31]:

$$\varepsilon_1 = \frac{\mathrm{Re}\{1/\varepsilon\}}{(\mathrm{Re}\{1/\varepsilon\})^2 + (\mathrm{Im}\{1/\varepsilon\})^2}\varepsilon_2 = \frac{\mathrm{Im}\{1/\varepsilon\}}{(\mathrm{Re}\{1/\varepsilon\})^2 + (\mathrm{Im}\{1/\varepsilon\})^2}. \quad (6)$$

Fig. 5(b) shows ε_1 and ε_2 (corresponding to the absorption spectrum) of the dielectric functions. The main peaks of ε_1 at 4.7, 4.4 and 4.5 eV before annealing increased to 5.1, 4.7 and 4.7 eV after annealing at 350 °C for IZTO-I, IZTO-II, and IZTO-III, respectively. The main peaks of ε_2 in Fig. 5(b) are at 5.6, 5.2, and 5.3 eV before annealing and increased to 6.0, 5.5 and 5.6 eV after annealing at 350 °C for IZTO-I, IZTO-II, and IZTO-III, respectively. This result implies that dielectric function resulted from a lower Sn content is smaller than that from a higher Sn content in the IZTO thin films. There is no change in the dielectric constant of IZTO-II and IZTO-III before and after annealing. Thus, the dielectric constants are independent of the amount of In contents in IZTO thin films.

The refractive index$n$ and extinction coefficient$k$ are determined from the dielectric function by using the following relations [31]:

$$n = \sqrt{\frac{1}{2}(\sqrt{\varepsilon_1^2 + \varepsilon_2^2} + \varepsilon_1)}\text{and}k = \sqrt{\frac{1}{2}(\sqrt{\varepsilon_1^2 + \varepsilon_2^2} - \varepsilon_1)}. \quad (7)$$

As shown in Fig. 6, the refractive index of IZTO thin films decreased with increasing wavelength.

The dispersion of the refractive index in terms of the energy dependence of amorphous IZTO thin films using REELS results can be fitted by a single-effective oscillator model. This method was suggested by the Wemple and DiDomenico dispersion relation model and can be expressed in the form [32,33]:

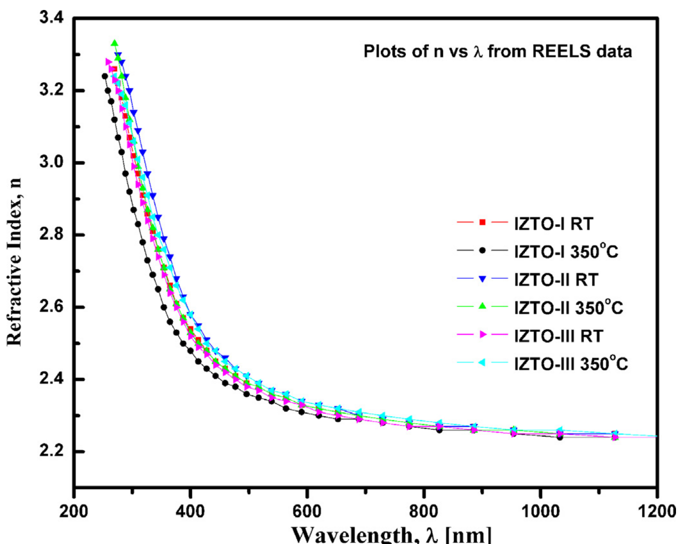

Fig. 6. The dispersion of refractive index (n) as a function of wavelength (λ) for IZTO thin films with different composition of In/Zn/Sn estimated by quantitative analysis of REELS.

$$n^2(E) - 1 = \frac{E_d E_0}{E_0^2 - E^2}, \quad (8)$$

where E_0, E_d, and E are the single-oscillator energy, dispersion energy (oscillator strength), and incident photon energy, respectively. Note that the dispersion energy (E_d) is related to the average strength of the inter-band optical transitions. In order to obtain E_o and E_d, we plotted $(n^2-1)^{-1}$ against E^2 and fitted the data with a straight line. Fig. 7(a) shows a plot of $(n^2-1)^{-1}$ versus E^2 for IZTO thin films with differing In content and In/Zn/Sn ratios for both before and after annealing. The values of E_0 and E_d can be estimated from the slope of $(E_0E_d)^{-1}$ and the intercept on the y-axis (E_0/E_d), respectively, and the results are listed in Table 2. The single-oscillator energy (E_0) has been reported as an empirical relationship with the direct band gap by $E_0 \approx 1.9\,E_g$ [34,35]. This relationship is consistent with our results obtained from the single-oscillator model based on REELS data for all IZTO thin films ($E_0 \approx 1.8\,E_g$). Table 2 shows that the values of E_0 and E_d for IZTO thin films are close to those of ZnO and SnO_2, respectively, which can be found elsewhere [36,37]. Note that the band gap of ZnO is much smaller than those of SnO_2 and In_2O_3 [38–40]. According to Wemple and Didomenico, the value of the oscillator energy is related to the lowest direct band gap [32]. Hence, the value of oscillator energy of IZTO decreased with increasing Sn/Zn ratios in comparison to IZTO-I and IZTO-II films. The results, as shown in Table 2, indicate that the oscillator energy E_0 is strongly influenced by the Zn content. However, the small differences in the oscillator energy E_0 between unannealed and annealed films of IZTO-II and IZTO-III show that the E_0 is not significantly affected by the In contents. On the other hand, the dependency of dispersion energy E_d on coordination number and chemical valence suggest that the nearest-neighbor atom-like quantities strongly affect the optical properties of TCO materials [32,34]. Wemple and DiDomenico reported the following relation between E_d and the physical parameters [35]:

$$E_d = \beta N_c Z a N_e, \quad (9)$$

where N_c is the number of nearest neighbor cations to the anion, Z_a is the formal chemical valence of the anion, and N_e is the effective number of electrons per single anion. Wemple and DiDemenico [32] reported that the parameter β is a constant having two different values of 0.26 ± 0.04 eV and 0.37 ± 0.05 eV for an ionic oxide compound and a covalent crystal, respectively. The value of for IZTO thin films with different In contents and Sn/Zn ratios are tabulated in Table 2. From these values it is apparent that for the IZTO films the β values are within the range known for ionic oxides. According to Eq. (9), the dispersion energy E_d is related to the value of N_c, N_e, and Z_a. The values of N_e and Z_a were fixed for IZTO thin films. Therefore, the decrease in the dispersion energy with increasing Zn contents in IZTO thin films is attributed to a decrease in coordination number.

The static refractive index (n_0) can be obtained by extrapolating the Wemple and DiDomenico dispersion relation as follows [32]:

$$n^2(0) = 1 + \frac{E_d}{E_0}. \quad (10)$$

The values of the zero – frequency dielectric constant (static dielectric constant), $\varepsilon_0 = n_0^2$ were calculated. We found that there is no significant difference between the static refractive index and the zero frequency dielectric constant with different In contents and Sn/Zn ratios. The value of n_0 calculated by this method is approximately 2.2 for all IZTO films. This value is in good agreement with the values obtained from the optical transmission data of UV-spectrometer by the Swanepoel method. Similarly, the values of the static dielectric constant from this method ($\varepsilon_0 \approx 5$) are

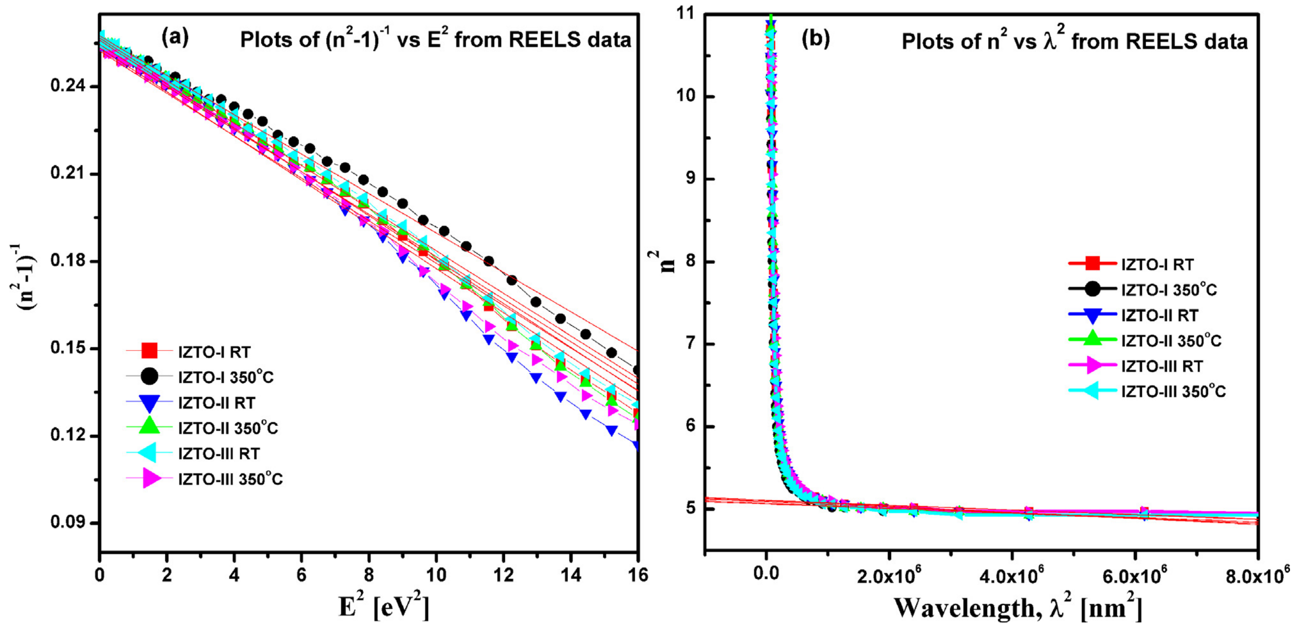

Fig. 7. (a) Plots of $(n^2-1)^{-1}$ as a function of E^2 and (b) plots of n^2 versus λ^2 for IZTO thin films with different In content and Sn/Zn ratios.

Table 2
The optical parameters for IZTO thin films with different In content and Sn/Zn ratios estimated by quantitative analysis of reflection energy loss spectroscopy.

Films	E_0(eV)	E_d(eV)	E_g (eV)	n_0	β	E_a (eV)	$\hbar\omega_p$ (eV)	ε_0	λ_0 (10^{-7} m)	S_o (10^{13} m^{-2})	$n=\sqrt{\varepsilon_L}$	ε_L	N/m^* (x 10^{47} g^{-1} cm^{-3})
IZTO-I-RT	5.96	23.19	3.36	2.219	0.242	1.89	6.63	4.93	2.09	8.91	2.243	5.033	10.88
IZTO-I-350 °C	6.17	23.95	3.54	2.209	0.249	2.03	7.00	4.88	2.01	9.58	2.237	5.006	9.11
IZTO-II-RT	5.74	22.80	3.20	2.223	0.237	1.77	6.36	4.95	2.15	8.58	2.237	5.007	9.00
IZTO-II-350 °C	5.83	22.76	3.42	2.214	0.237	2.01	6.76	4.91	2.13	8.62	2.235	4.997	7.84
IZTO-III-RT	5.80	23.31	3.15	2.228	0.243	1.69	6.27	4.96	2.11	8.93	2.245	5.041	11.90
IZTO-III-350 °C	5.93	23.08	3.31	2.212	0.240	1.85	6.53	4.89	2.09	8.90	2.237	5.008	9.63
SnO_2	8.24[a]	23.92[a]	3.60[b]	2.094[a]	–	–	–	–	–	–	–	–	–
In_2O_3	6.34[a]	18.99[a]	3.70[b]	2.093[a]	–	–	–	–	–	–	–	–	–
ZnO	5.79[a]	15.19[a]	3.37[b]	2.023[a]	–	–	–	–	–	–	–	–	–

[a] The oscillator parameters determined by the crystal prism method including refractive indices are taken from the Ref. [36] for SnO_2 and [37] for ZnO and In_2O_3.
[b] The band gap values for ZnO, SnO_2, and In_2O_3 are taken from the Ref. [38],[39], and [40], respectively.

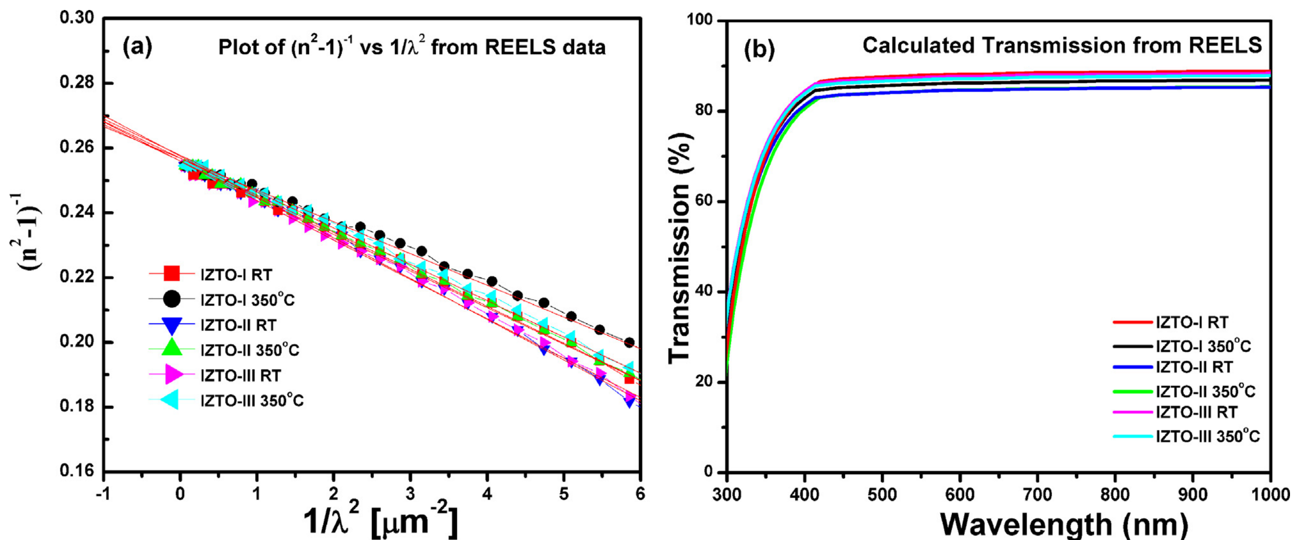

Fig. 8. (a) Plot of $(n^2-1)^{-1}$ as a function of $1/\lambda^2$ and (b) calculated transmission spectra for IZTO thin films from REELS results.

consistent with the values estimated by REELS data (see Fig. 5 (b) at zero energy loss). The values of static refractive indices and zero frequency dielectric constant estimated by Wemple-DiDomenico dispersion relation is given in Table 2.

The relation between the lattice dielectric constant ε_L and refractive index n is given by [41]:

$$n^2 = \varepsilon_L - \left(\frac{e^2}{\pi c^2}\right)\left(\frac{N}{m*}\right)\lambda^2, \quad (11)$$

where ε_L, e, N/m^* are the lattice dielectric constant, elementary charge, and ratio of carrier concentration to the effective mass, respectively. Plots of n^2 versus λ^2 of IZTO thin films are shown in Fig. 7(b). The values of ε_L and N/m^* listed in Table 2 can be estimated from the intersection of the straight line with $\lambda^2 = 0$ and from the slopes of the line, respectively. The obtained values of the N/m^* ratios from IZTO thin films with different In contents and Sn/Zn ratios were in the range between 9.0×10^{47} and 12.0×10^{47} $g^{-1}\,cm^{-3}$. These results are in good agreement with those obtained by the free carrier absorption (FCA) method [42]. The results obtained from the preliminary analysis of the lattice dielectric constant ε_L are consistent with the calculated value of the static dielectric constant ε_0.

Furthermore, the band gap parameter E_a introduced by Hopfield [43] was calculated to get a better understanding of the optical properties. This parameter gives the connection between a single-oscillator parameter and the Philips parameters in the following expression [44]:

$$E_0 \cdot E_a = E_g^2 \text{and} E_a \cdot E_d = (\hbar\omega_p)^2. \quad (12)$$

The calculated band gap parameter E_a and the plasma oscillator energy $\hbar\omega_p$ for IZTO thin films with different In contents and Sn/Zn ratios are shown in Table 2. Notice that the plasma oscillation frequency (ω_p) is the natural frequency for the free conduction electron due to vibrations which can be observed experimentally. In the REELS experiment, any electrons passing through a solid with a sufficient energy can excite one or other modes of the collective oscillations of conduction electrons. From Table 2, we can see that the optical values of the plasmon energy $\hbar\omega_p$ calculated using the Hopfield method are close to the first plasmon peak from the REELS. Hence, the method using a single-oscillator analysis can be employed only for the first plasmon peak calculations in the REELS experiment.

From the dispersion of the refractive index n, one can determine the average interband oscillator wavelength (λ_0) and the average oscillator strength (S_0) for all films with differing In contents and Sn/Zn ratios (both before and after annealing) using a single Sellmeier oscillator in the following [44]:

$$(n^2 - 1) = \frac{S_0\lambda_0^2}{1 - \left(\frac{\lambda_0}{\lambda}\right)^2}. \quad (13)$$

The curves of $(n^2 - 1)^{-1}$ against λ^{-2} are plotted in Fig. 8(a) and the data are fitted with a straight line. The values of S_0 and λ_0 are obtained from the slope $(-1/S_0)$ and the infinite wavelength intercept $\left(1/S_0\lambda_0^2\right)$, respectively, which are listed in Table 2. Another method given by $E_0 = hc/q\lambda_0$ (h is Plank's constant, c the light velocity, and q the charge of the electron) and $E_d = E_0S_0\lambda_0^2$ was used to confirm the value of S_0 and λ_0 [45]. It is found that the results are consistent with each other (the values are not shown). In Table 2, we can see that S_0 increases with increasing Sn and In contents in the IZTO thin films. In addition, the obtained values of λ_0 and S_0 are in the same order as those obtained by Wemple and Didemenico for a number of materials [32].

In our work, we also determined the calculated transmission coefficient T from the relation $R + T + \mu = 1$, where R is the reflection coefficient given by the relation [31]:

$$R = \frac{(n-1)^2 + K^2}{(n+1)^2 + K^2}, \quad (14)$$

and μ is the absorption coefficient related to the extinction coefficient k as follows:

$$\mu = 10.1 \cdot habaromwga \cdot K, \quad (15)$$

where $\hbar\omega$ is the energy loss.

Fig.8(b) shows the calculated transmittances as a function of wavelength for IZTO thin films. In the visible light region, the transmittance coefficients are approximately 87% for all films without a change due to the Zn contents and annealing treatment. We measured the spectral transmittances of all IZTO thin films using a UV-Spectrometer with the wavelength ranging from 300 to 1000 nm to compare with the calculated transmittances from REELS as shown in Fig. 3(a). As shown in Fig. 8(b), no interference fringes were observed in the calculated transmittances spectra from REELS. The REELS is a surface sensitive tool and only experiences the local investigation of the optical properties in the topmost few monolayers of the film. Hence, the REELS results do not depend on the roughness of the films. The interference fringes in the UV-spectrometer are not present in the REELS results. Overall, the values of the transmission coefficient are consistent for both methods: for data calculated from REELS spectra and for data obtained using a UV-Spectrometer.

4. Conclusion

The electronic properties and optical parameters of IZTO thin films were investigated by REELS. We found that the band gap of IZTO thin films increased with increasing Sn/Zn ratios in the films and increased after annealing at 350 °C in air. Furthermore, the band gap increased with increasing In contents. The optical constants were obtained from the measured transmittance spectra using the envelope method. In addition, the dispersion behavior and the oscillator parameters obtained from the REELS data were determined using a single-oscillator of Wemple-DiDomenico model. The results of this study indicate that the Zn and Sn contents play a crucial role in determining the single-oscillator constant and dispersion energy of IZTO thin films. The electronic properties were improved by a lower content of In in IZTO thin films, and different In/Zn/Sn compositions had no effect on the optical transmittance of IZTO thin films.

Acknowledgments

The authors would like to thank Prof. Dong Hyun Kim and Mr. Djati Handoko from Physics Department at Chungbuk National University for the AFM measurement and discussions. The authors also would like to thank to the Ministry of Education and Culture, Indonesian Goverment in terms of Hibah Penelitian Strategi Nasional 2015. This research was supported by the Basic Science Research Program through the National Research Foundation of Korea (NRF) funded by the Ministry of Education, Science and Technology (2012R1A1A2009590).

References

[1] M.S. Grover, P.A. Hersh, H.Q. Chiang, E.S. Kettenring, J.F. Wager, D.A. Keszler, J. Phys. D: Appl. Phys. 40 (2007) 1335.
[2] D.H. Lee, S.Y. Han, G.S. Herman, C.H. Chang, J. Mater. Chem. 19 (2009) 3135.
[3] M.G. Kim, H.S. Kim, Y.G. Ha, J. He, M.J. Kanatzidis, A. Facchetti, T.J. Mark, J. Am. Chem. Soc. 132 (2010) 30.

[4] G.S. Heo, I.G. Gim, J.W. Park, K.Y. Kim, T.W. Kim, J. Solid State Chem. 182 (2009) 2937.
[5] Y.D. Ko, Y.S. Kim, Mater. Res. Bull. 47 (2012) 2800.
[6] D.H. Kim, C.H. Choi, S.J. Park, H.H. Yoon, K.H. Kim, Mol. Cryst. Liq. Cryst. 532 (2010) 91 507.
[7] H.K. Park, J.A. Jeong, Y.S. Park, H.K. Kim, W.J. Cho, Thin Solid Films 517 (2009) 5563.
[8] T. Minami, T. Kakumu, K. Shinokawa, S. Takata, Thin Solid Films 317 (1998) 318.
[9] Y. Shen, D.B. Jacob, G.G. Malliaras, G. Koley, M.G. Spencer, A. Ioannidis, Adv. Mater. 13 (2001) 1234.
[10] H.C. Damisih, Ma, J.J. Kim, H.Y. Lee, Thin Solid Films 520 (2012) 3741.
[11] K.J. Saji, M.K. Jayaraj, Thin Solid Films 516 (2008) 6002.
[12] R.F. Egerton, Electron Energy-Loss Spectroscopy the Electron Microscopy, second ed., Plenum, New York, 1996.
[13] S. Tougaard, F. Yubero, QUEELS-ε(k,ω)-REELS: Quantitative Analysis of Electron Energy Loss Spectra: Dielectric Function Determined by Reflection Electron Energy Loss Spectroscopy, version 3, (2008)
[14] A.M. Nasr, H.I. Abd El-Kader, M. Farhat, Thin Solid Films 515 (2006) 1758.
[15] C. Caliendo, E. Verona, G. Saggio, Thin Solid Films 292 (1997) 255.
[16] A.M. Nasr, A.M. Sadik, J. Opt. A Pure Appl. Opt. 3 (2001) 200.
[17] S. Hajati, O. Romanyuk, J. Zemek, S. Tougaard, Phys. Rev. B 77 (2008) 155403.
[18] Y.R. Denny, H.C. Shin, S. Seo, S.K. Oh, H.J. Kang, D. Tahir, S. Heo, J.G. Chung, J.C. Lee, S. Tougaard, J. Elect. Spect. Rel. Phenom. 185 (2012) 18.
[19] Y.R. Denny, S. Lee, K. Lee, S. Seo, S.K. Oh, H.J. Kang, S. Heo, J.G. Chung, J.C. Lee, S. Tougaard, Vac. Sci. Technol. A 31 (3) (2013) 031508.
[20] D.L. Wood, J. Tauc, Phys. Rev. B 5 (1972) 3144.
[21] Y.R. Denny, S. Lee, K. Lee, S. Seo, S.K. Oh, D.S. Yang, H.J. Kang, S. Heo, J.G. Chung, J. C. Lee, Appl. Surf. Sci. 315 (2014) 454.
[22] E. Burnstein, Phys. Rev. 93 (1954) 632.
[23] J.C. Manifacier, J. Gasiot, J.P. Fillard, J. Phy. E: Sci. Instrum. 9 (1976) 1002.
[24] R. Swanepoel, J. Phy. E: Sci. Instrum. 16 (1983) 1214.
[25] M. Sreemany, S. Sen, Mater. Chem. Phys. 83 (2004) 169.
[26] S. Tougaard, I. Chorkendorff, Phys. Rev. B 35 (1987) 6570.
[27] F. Yubero, D. Fujita, B. Ramskov, S. Tougaard, Phys. Rev. B 53 (1996) 9728.
[28] S. Tougaard, F. Yubero, Surf. Interf. Anal. 36 (2004) 824.
[29] D. Pines, P. Nozieres, The Theory of Quantum Liquids, vol. 1, W. A. Benjamin, New York, 1996.
[30] G.L. Tan, L.K. DeNoyer, R.H. French, M.J. Guittet, M. Gautier-Soyer, J. Elect. Spect. Rel. Phenom. 142 (2004) 97.
[31] F. Wooten, Optical Properties of Solid, Academic Press, New York, 1972.
[32] S.H. Wemple, M. DiDemenico, Phys. Rev. B 3 (1971) 1338.
[33] J. Tauc, The Optical Properties of Solids, North-Holland, Amsterdam, 1970.
[34] S. Goldsmith, E. Çetinörgü, R.L. Boxmann, Thin Solid Films 517 (2009) 5146.
[35] K. Tanaka, Thin Solid Films 66 (1980) 271.
[36] R.D. Shannon, R.C. Shannon, O. Medenbach, R.X. Fischer, J. Phys. Chem. Ref. Data 31 (2002) 2762.
[37] O. Medenbach, T. Siritanon, M.A. Subramanian, R.D. Shannon, R.X. Fischer, G.R. Rossman, Mater. Res. Bull. 48 (2013) 2240.
[38] A. Janotti, C.G.V. Walle, Rep. Prog. Phys. 72 (2009) 126501.
[39] M.A. Mäki-Jaskari, T.T. Rantala, Phys. Rev. B 64 (2001) 075407.
[40] F. Fuchs, F. Bechstedt, Phys. Rev. B 77 (2008) 155107.
[41] J. Robert, A. Mark, W. Alexander, J. Appl. Optics 24 (1985) 3680.
[42] K.J. Saji, M.K. Jayaraj, K. Nomura, T. Kamiya, H. Hosono, J. Electrochem. Soc. 155 (2008) H390.
[43] J. Hopfiels, J. Phys. Rev. B 2 (1970) 973.
[44] M. DiDomenico, S.H. Wemple, J. Appl. Phys. 40 (1969) 720.
[45] A.M. Salem, T.M. Dahy, Y.A. El-Gendy, Physica B 403 (2008) 3027.